Biochimica et Biophysica Acta 1863 (2017) 817–826

Contents lists available at ScienceDirect

Biochimica et Biophysica Acta

journal homepage: www.elsevier.com/locate/bbadis

Molecular pathogenicity of novel sucrase-isomaltase mutations found in congenital sucrase-isomaltase deficiency patients

Birthe Gericke [a,1], Mahdi Amiri [a,1], C. Ronald Scott [b], &, Hassan Y. Naim [a,*]

[a] Department of Physiological Chemistry, University of Veterinary Medicine Hannover, Germany
[b] Department of Pediatrics, University of Washington, Seattle, WA 98195, USA

ARTICLE INFO

Article history:
Received 13 October 2016
Received in revised form 15 December 2016
Accepted 30 December 2016
Available online 3 January 2017

Keywords:
Sucrase-isomaltase
Carbohydrate malabsorption
Genetic intestinal disorders
Protein trafficking

ABSTRACT

Background & aims: Congenital sucrase-isomaltase deficiency (CSID) is a genetic disorder associated with mutations in the *sucrase-isomaltase* (*SI*) gene. The diagnosis of congenital diarrheal disorders like CSID is difficult due to unspecific symptoms and usually requires invasive biopsy sampling of the intestine. Sequencing of the *SI* gene and molecular analysis of the resulting potentially pathogenic SI protein variants may facilitate a diagnosis in the future. This study aimed to categorize SI mutations based on their functional consequences.
Methods: cDNAs encoding 13 SI mutants were expressed in COS-1 cells. The molecular pathogenicity of the resulting SI mutants was defined by analyzing their biosynthesis, cellular localization, structure and enzymatic functions.
Results: Three biosynthetic phenotypes for the novel SI mutations were identified. The first biosynthetic phenotype was defined by mutants that are intracellularly transported in a fashion similar to wild type SI and with normal, but varying, levels of enzymatic activity. The second biosynthetic phenotype was defined by mutants with delayed maturation and trafficking kinetics and reduced activity. The third group of mutants is entirely transport incompetent and functionally inactive.
Conclusions: The current study unraveled CSID as a multifaceted malabsorption disorder that comprises three major classes of functional and trafficking mutants of SI and established a gradient of mild to severe functional deficits in the enzymatic functions of the enzyme.
General significance: This novel concept and the existence of mild consequences in a number of SI mutants strongly propose that CSID is an underdiagnosed and a more common intestinal disease than currently known.

1. Introduction

About 70% of the human population is affected by some form of carbohydrate malabsorption [1]. Malabsorption of carbohydrates can result from genetic or environmental factors that inhibit the catalytic activity of intestinal disaccharidases. Sucrase-isomaltase (SI) [2], maltase-glucoamylase (MGAM) [3] and lactase-phlorizin hydrolase (LPH) [4] are the prominent intestinal disaccharidases, which contribute to the final step of carbohydrate breakdown. SI is predominantly expressed at the apical membrane of enterocytes. The isomaltase subunit of SI is the major enzyme for cleavage of branched α-1,6-linkages while the sucrase subunit of SI mainly hydrolyses α-1,2-glucosidic bonds of sucrose.

Functionally, the combined units account for 60% to 80% of maltose digestion [5–7]. The SI protein is translated, folded and N-glycosylated in the ER (SI_h, ~210 kDa) and transported from the ER to the Golgi apparatus where complex N- and O-glycosylation takes place. The mature protein (SI_c, ~245 kDa) is then transported *via* cholesterol- and sphingolipid-enriched membrane microdomains mainly to the apical cell surface [8].

Genetic defects of *SI* can lead to congenital sucrase-isomaltase deficiency (CSID) [9,10]. Patients with this disorder show a substantial reduction or absence of the sucrase and/or isomaltase activities linked to reduced digestive capacity of the small intestine in general [11]. The failure of digestion and impaired absorption of maldigested carbohydrates triggers osmotic diarrhea. The patients may also suffer from vomiting, flatulence or abdominal pain ranging from mild to severe [11,12]. Occasionally dehydration, failure to thrive, developmental retardation and muscular hypotonia have been observed [12,13]. The maldigestion of sugars can also affect the absorption of other nutrients and can influence the hormonal regulation of the intestinal function [12,14]. The chronic malabsorption of carbohydrates can lead to malnutrition in CSID patients [15]. Common symptoms of CSID with other congenital diarrheal

Abbreviations: CSID, congenital sucrase-isomaltase deficiency; SI, sucrase-isomaltase; SUC, sucrase; IM, isomaltase; endo H, *endo*-β-*N*-acetylglucosaminidase H.

* Corresponding author at: Department of Physiological Chemistry, University of Veterinary Medicine Hannover, D-30559, Hannover, Germany.
E-mail address: hassan.naim@tiho-hannover.de (H.Y. Naim).

[1] These authors contributed equally to this work.

http://dx.doi.org/10.1016/j.bbadis.2016.12.017
0925-4439/

disorders like congenital lactase deficiency [16] and glucose-galactose malabsorption [17] or with secondary acquired intestinal disorders like inflammation and food allergies [18,19] complicate the diagnosis and therapy of CSID [20]. A univocal diagnosis of CSID mostly requires invasive biopsy sampling of the patients and subsequent analysis of disaccharidase activities and intestinal histology [11,21].

Mutations in the coding region of the *SI* gene are the major cause of CSID [22,23]. Genetically altered SI protein may exhibit perturbations in intracellular transport, polarized sorting and abnormal processing [24–26].

Population studies have estimated the frequency of CSID as 0.2% of individuals of European descents, 5% to 10% in indigenous Greenlanders and 3% to 7% of Inuits of Alaska and Canada [12,27–30]. Four common mutations, p.G1073D, p.V577G, p.F1745C and p.R1124X, are suggested to account for 83% of disease alleles in European descendants diagnosed with CSID. Gene sequencing and molecular analysis in patients with suspected CSID can help to identify pathogenic protein variants and aid to functionally categorize SI mutations. This may facilitate a diagnosis and subsequent earlier treatment of CSID.

Some of the naturally occurring SI mutants have been previously identified and characterized at the molecular level by our group [10,31–33].

In the present study we revealed the molecular pathogenesis in a selection of 13 novel SI mutations from patients with confirmed biopsy diagnosis of CSID and defined three biosynthetic phenotypes according to the molecular pathogenicity of the respective mutation. The analyzed mutations also included the R1124X mutation, which is described as one of the four most common mutations in European descents. The *in vitro* pathogenicity was determined based on the effect of the mutation on the SI functionality. Therefore we expressed cDNAs, encoding the different SI mutants, in a COS-1 cell system and analyzed the biosynthesis, structure and enzymatic activity of the SI protein variants.

2. Materials and methods

2.1. Materials and reagents

Tissue culture dishes were obtained from Sarstedt (Nüembrecht, Germany). Dulbecco's Modified Eagle's Medium (DMEM), methionine-free DMEM, penicillin, streptomycin, fetal calf serum, trypsin-EDTA for cell culture, protease inhibitors, DEAE-dextran, protein A-sepharose, trypsin, and Triton X-100 were purchased from Sigma-Aldrich (Deisenhofen, Germany). Acrylamide, TEMED, SDS, Tris, paraformaldehyde, dithiothreitol (DTT), polyvinyl difluoride (PVDF) membrane, ProLong Gold Antifade Reagent with DAPI, as well as sucrose and isomaltose were purchased from Carl Roth GmbH (Karlsruhe, Germany). [^{35}S]-methionine (>1000 Ci/mmol) was obtained from PerkinElmer (Waltham, Massachusetts). Glucose oxidase-peroxidase mono-reagent was obtained from Axiom GmbH (Bürstadt, Germany). Restriction enzymes, molecular weight standards for SDS-PAGE, Isis proofreading DNA polymerase and SuperSignal™ West Fermento maximum sensitivity western blot chemiluminescence substrate were obtained from Thermo Fisher Scientific GmbH (Schwerte, Germany). Endo-β-*N*-acetylglucosaminidase H (endo H) was acquired from Roche Diagnostics (Mannheim, Germany). Lubrol WX was purchased from MP Biomedicals (Eschwege, Germany). All other reagents were of superior analytic grade.

2.2. Immunochemical reagents

The monoclonal mouse anti-SI antibodies (mAb) hSI2, HBB1/691/79, HBB2/614/88, HBB2/219/20, and HBB3/705/60 [34,35] were kindly provided by Dr. H.P. Hauri and Dr. E.E. Sterchi (Bern, Switzerland). To recognize all conformations and glycoforms of the SI mutants a mixture of these antibodies was used for immunoprecipitation. Anti-calnexin antibody produced in rabbit was obtained from Sigma-Aldrich Chemie GmbH (Munich, Germany). Secondary antibodies coupled to Alexa Fluor dyes were obtained from Invitrogen (Karlsruhe, Germany) and horseradish peroxidase conjugated secondary antibodies were from Thermo Fisher Scientific (Schwerte, Germany).

2.3. Recruitment of CSID patients and identification of mutations in the SI gene

A total of 31 probands with a confirmed biopsy diagnosis of CSID were recruited by different attempts, including a letter to gastroenterologists, booth and literature at gastroenterology meetings, package inserts in Sucraid boxes, and notices on patient listservs by families participating in the study. All patients had bowel biopsies with normal lactase but reduced or absent sucrase and/or isomaltase activities and a normal histology. DNA analysis was performed with patient consent and IRB approval. DNA for sequencing of the entire *SI* gene coding region was extracted from blood or saliva of the patients. DNA sequencing was performed by Sanger dideoxy sequencing [36] using an ABI Prism 3130xl genetic analyzer (Applied Biosystems, Carlsbad, CA). The sucrase-isomaltase exons and flanking introns were compared to the GeneBank number NM_001041.3 to detect nucleotide alterations [30].

2.4. Construction of cDNA clones

SI mutations were generated by site-directed mutagenesis PCR using a full length cDNA encoding SI in a pSG8 vector as template [37] and Isis proofreading polymerase for the PCR amplification. Sequences of single strand oligonucleotide pairs used for mutagenesis are presented in Table 1. For analytical digestion of the resulting clones particular restriction sites were introduced or deleted in the vicinity of the target site by silent mutations within the oligonucleotide pairs. SI mutations were finally validated by Sanger sequencing.

Table 1
Sequence of the forward oligonucleotides used for mutagenesis PCR of SI wild type. The reverse oligonucleotides have the reverse complementary sequence. The mutagenic base pair codons are underlined and the corresponding amino acids are listed below.

SI mutants	Oligonucleotide sequences used for mutagenesis (5′–3′)
W105C	CGTGGAATGACTCTCTTATTCCTGTTGCTTCTTCGTTGATAATCATG Cys
F139Y	CCTTCACCTACACTATACGGAAATGATATCAACAGTGTTC Tyr
Q307Y	GTTTTTTTAATGAATTCCAACGCAATGGAGATTTTTATCTATCCTACACCAAT AGTAAC Tyr
D536V	CACCGTTTACTCCTGATATCCTTGTCAAACTCATGTATTCCAA Val
S594P	CTCAACATTTGCTGGTCCTGGTCGACATGCTGCTCATTGG Pro
L741P	CTGAGTTTTTGTGGGGACCTGCATTACCTATTACTCCTGTTCTA Pro
Q930R	GAAACTTTAGTGTTCGATGGAATCAGATCTTCTCAGAAAATG Arg
W931R	GCAGATCTCAAGCTTAATCTCGGAAGAAACTTTAGTGTTCAACGGAATCAAA TTT Arg
W931X	CTTTAGTGTTCAATAGAATCAGATCTTCTCAGAAAATGA Stop
R1124X	GAACATACAGCATTTAAGTGATATCTGAACTGGAATAC Stop
C1531Y	TGTTTGGAATGTCATATACTGGGCAGATATCTATGGTTTTTTCAACAACTC Tyr
R1544C	GAATATCATCTCTGTACCTGTTGATGCAGCTGGGAGCATTTTATCCA Cys
T1606I	CATGAAATTCATGCTAATGGTGGCATTGTTATCCG Ile

2.5. Cell culture, transient transfection and biosynthetic labeling

COS-1 cells were grown in 100-mm culture dishes and maintained *in vitro* by serial passages at 37 °C in a humidified atmosphere with 5% CO_2. The cells were cultivated in DMEM containing 1 g/L glucose, 10% fetal calf serum (*v*/*v*), 100 U/mL penicillin and 100 μg/mL streptomycin. Transient transfection of the cells was performed by the DEAE-dextran method as described previously [38]. The COS-1 cells were used 48 h post-transfection for different analyses including biosynthetic labeling with [^{35}S]-methionine as described before [39].

2.6. Cell lysis and immunoprecipitation

Solubilization of the cells and immunoprecipitation of SI from the lysates has been essentially performed as described previously [2,40,41]. For endoglycosidase studies, the immunoprecipitants were subjected to *endo*-β-*N*-acetylglucosaminidase H (endo H) treatment as described before [2].

2.7. SDS-PAGE and protein detection

Cell lysates or immunoprecipitants of unlabeled samples were mixed with Laemmli buffer and DTT, cooked 5 min at 95 °C and resolved on 6% slab gels. After protein transfer to the PVDF membrane, immunedetection of SI was performed by either HBB2/614/88 (recognizing the sucrase subunit) or HBB3/705/60 (recognizing the isomaltase subunit) primary antibodies followed by HRP-conjugated secondary antibody incubation and washing steps after each incubation. The corresponding bands were detected by a ChemiDoc XRS System (Bio-Rad, Munich, Germany) after addition of chemiluminescent substrate. The radioactive labeled samples were similarly resolved on SDS-PAGE, dried on filter papers, exposed to phosphor plates and detected by a phosphor imager (Bio-Rad, Munich, Germany).

2.8. Isolation of detergent-resistant membrane microdomains

Transiently transfected COS-1 cells were solubilized at 4 °C for 4 h with 1% Lubrol WX or Triton X-100 in 10 mM Tris buffer pH 8.0 with 150 mM NaCl. Lipid rafts were isolated using sucrose discontinuous gradient as described before [42]. Fractions of 1 mL were collected from top and denoted 1 to 10. For SDS-PAGE analysis, a part from fractions 1 to 3, 4 to 7 and 8 to 10 was pooled separately and the proteins were extracted and precipitated using chloroform-methanol precipitation [43]. The protein pellet was dissolved in Laemmli buffer plus DTT, resolved on SDS-PAGE and immunoblotted for SI, flotillin-2 and Rho A proteins.

2.9. Enzyme activity measurements

Immunoprecipitants of SI were washed with PBS containing 0.5% Triton X-100 and split to two equal parts. One part was incubated with either sucrose (150 mM) or isomaltose (30 mM) substrate for 1 h at 37 °C to measure the enzyme activity. Activities were calculated based on the detection of the released glucose by adding glucose oxidase-peroxidase mono-reagent and measuring of 492 nm absorbance with a microplate reader. The second part of the immunoprecipitants was used for immunoblotting against SI. The intensity of the SI signal in each sample was quantified and normalized to the band intensity of the wild type sample. Relative specific activities were determined by dividing the enzyme activities to the relative protein intensities.

2.10. Confocal fluorescence microscopy

COS-1 cells were seeded on coverslips, transfected with SI constructs and fixed 48 h post-transfection with 4% paraformaldehyde. The samples were prepared as described before [44] using a combination of mouse anti-SI primary antibodies to detect SI and rabbit anti-calnexin antibody as an ER marker. ProLong Gold Antifade Reagent with DAPI was used to visualize the cell nucleus and for mounting of the coverslips. The samples were examined by a Leica TCS SP5 confocal microscope with a HCPL APO 63 × 1.3 glycerol immersion objective.

2.11. Tryptic structural analysis

Transfected COS-1 cells were labeled for 6 h with [^{35}S]-methionine. Then SI was immunoprecipitated, washed and treated with 500 BAEE units of trypsin for 1 h at 37 °C. The reaction was stopped by the addition of Laemmli buffer plus DTT and cooking for 5 min at 95 °C. The samples were finally analyzed by SDS-PAGE. For differential identification of the bands corresponding to the sucrase or the isomaltase subunit, lysates of unlabeled cells were similarly treated with trypsin and subjected to immunoblotting with either HBB2/614/88 or HBB3/705/60 antibodies to visualize sucrase or isomaltase subunits, respectively.

2.12. Bioinformatic and statistical analysis

Alignment of the SI sequences has been performed by PRofile ALIgNEment (PRALINE) multiple sequence alignment application [45]. Immunoblot bands were quantified by the Quantity One 1-D Analysis Software (Bio-Rad Laboratories GmbH). Data analysis was performed by Microsoft Excel and the indicated error bars were calculated according to the standard error of the mean (SEM) from at least three independent repeats. Results are expressed as means ± SEM of $n \geq 3$ independent experiments. Statistical analysis was performed using paired Student *t*-test compared to a wild type control. *$p < 0.05$; **$p < 0.01$; ***$p < 0.001$.

3. Results

3.1. Description of the SI mutations

The focus of this study was to define the molecular pathogenicity of 13 missense mutations in the *SI* gene. Therefore the functional influence of the genetic defect on the resulting SI protein variant was analyzed *in vitro*. The 13 mutations were among 56 different abnormal alleles, which were identified by screening the entire *SI* gene coding region in 31 patients with confirmed small bowel biopsy diagnosis of CSID [30]. Pathogenic variants identified in individuals with clinical symptoms were selected for this study. All individuals were of Northern European ethnic background, had symptoms of abdominal bloating, pain and diarrhea when ingesting complex carbohydrates. Duodenal biopsies were performed to document the enzymatic deficiency of sucrase and isomaltase in tissue samples (Table 2). The biopsies from the patients revealed no histological changes and reduced or absent enzymatic activities of isomaltase and sucrase [30]. Pathogenic variants were subsequently identified in DNA isolated from peripheral blood. All of the mutations were found to be inherited in a compound heterozygous pattern (Table 2). For the mutations Q307Y, F139Y and S594P no *ex vivo* data are available. All amino acid exchanges targeted motifs of the SI protein which are highly conserved among different species, indicating the structural or functional importance of these regions (Fig. 1).

3.2. Biosynthetic studies reveal three trafficking-relevant classes of SI mutants

Investigation of the maturation of each individual SI variant from the mannose-rich glycosylated SI precursor protein (SI_h, ~210 kDa) to its complex N- and O-glycosylated mature form (SI_c, ~245 kDa) in transiently transfected COS-1 cells led to the identification of three distinct biosynthetic phenotypes of the novel mutants. After 8 h of biosynthetic labeling 70% of the SI wild type protein was complex glycosylated and reached the Golgi apparatus or the cell surface (Fig. 2). SI variants

Table 2
Comparison of the activities of purified SI mutants *versus* their counterparts in the patients' intestinal biopsy specimens. The individual SI mutants were immunoprecipitated and their activities towards sucrose and isomaltose were measured. These activities are shown as a percentage of the SI wild type activities. Activities of SI in the biopsy specimens were measured using sucrose and palatinose (instead of isomaltose) and are shown in units. All studied sucrase-isomaltase mutations were found in a compound heterozygote background of inheritance.
References for sucrase (35–131 U) and isomaltase (32–139 U) activities are according to Dahlqvist [60], palatinose (3.8–41.54 U) activities are according to Gupta [61].

	Biosynthetic phenotype	Sucrase	Isomaltase/palatinase
L741P	III	5	6
F1745C	III	0	0
Patient		0	0
R1124X	III	0	0
G1073D	III	0	4
Patient		0	2
D536V	I	58	5.6
V577G	III	0	0
Patient		0	0
W105C	I	30	61
W931X	III	0	0
Patient		2.61	7.17
G1073D	III	0	4
C1531Y	II	7	109
Patient		5.9	3.5
Q930R	I	80	58
R1544C	III	3	71
Patient		15.3	22.5
W931R	III	0	11
T1606I	III	19	76
Patient		0	0

grouped in the first biosynthetic phenotype (W105C, F139Y, D536V and Q930R) mature in the cell at essentially similar maturation rates to the wild type SI. A proportion of 50% to 70% of total SI is present as the mature complex glycosylated protein after 8 h of labeling (Fig. 2). In two other SI protein variants (Q307Y and C1531Y) the genetic alteration elicited a partial and delayed maturation of SI with low amounts of complex glycosylated protein after 8 h of labeling. These SI variants were grouped in a second biosynthetic phenotype. A third biosynthetic phenotype was caused by SI variants (S594P, L741P, W931R, R1544C and T1606I) that do not traverse the Golgi and persist as mannose-rich glycosylated proteins concomitant with their block in the early secretory pathway, most likely in the ER (Fig. 2). The third phenotype comprised also two stop codon mutations, R1124X and W931X. These mutations resulted in truncated protein variants that revealed no sucrase subunit and respectively only a small part of the isomaltase subunit (Fig. 2). The R1124X variant was even not detectable by all our monoclonal antibodies utilized under native conditions, indicating a severe malfolding. Both SI variants are likely targeted to ER associated degradation.

The cellular localization of the SI mutants was found to be concomitant with the biosynthetic labeling data representing three classes with (i) strong Golgi-like and cell surface appearance of SI, (ii) partial Golgi-like localization, and (iii) complete co-localization with calnexin and ER arrest (Fig. 3).

As shown in Fig. 4, tryptic profiles of the SI mutant varied from a complete or partial degradation to a wild type-like cleavage pattern. The results are summarized in Table 3. Notably, misfolding as represented by the level of sensitivity to trypsin has a direct association with trafficking arrest in the ER and loss of function.

From the *trans*-Golgi network, the sorting of SI to the apical cell surface requires association with membrane microdomains or, lipid rafts, as a trafficking platform [8]. We examined the association of the SI mutants with lipid microdomains to seek for any correlation between the mutation and biosynthetic phenotype in terms of the trafficking and ultimately function. Fig. 5 demonstrates that SI mutants that have

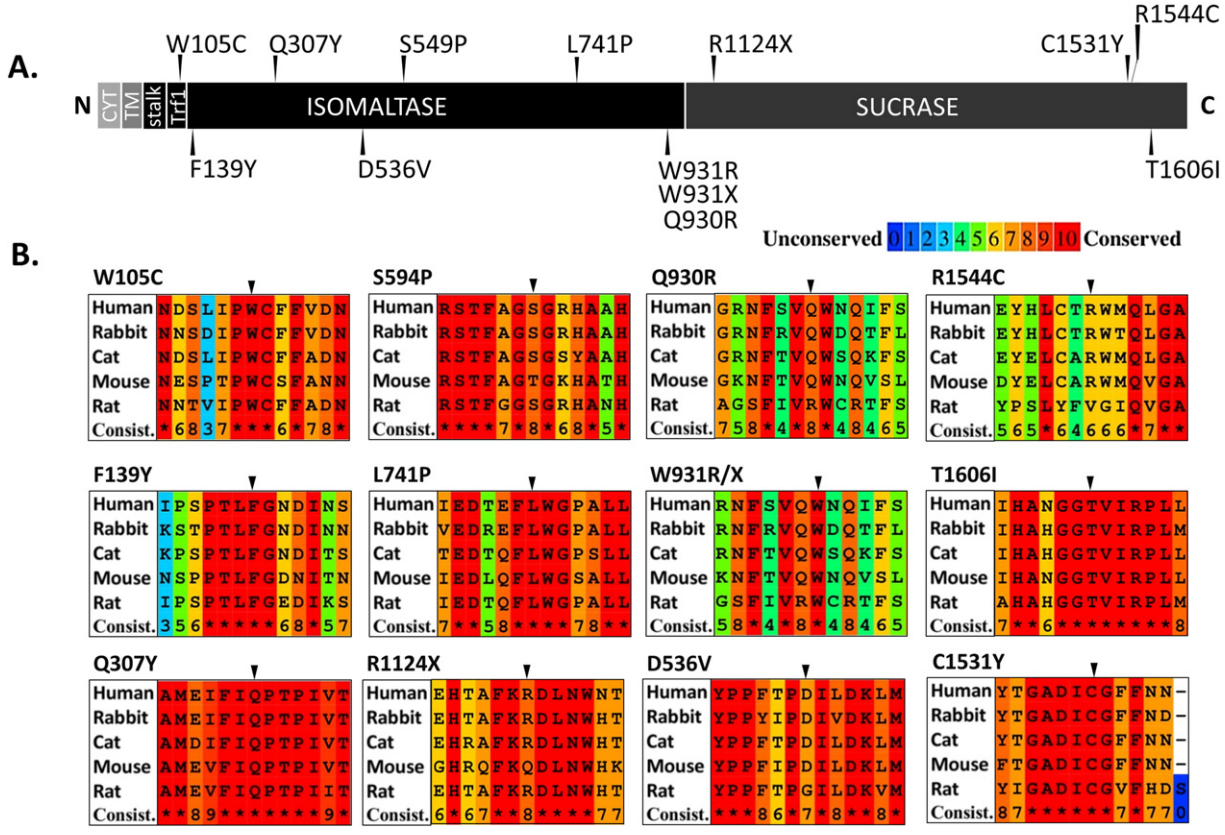

Fig. 1. The mutations studied target mainly highly conserved amino acid residues in consensus motifs of SI. (A) Schematic presentation of the position of the mutations within the SI molecule. CYT: cytosolic tail, TM: transmembrane domain, Trf1: trefoil 1. (B) Homology-extended multiple sequence alignment of the primary structure of SI among different mammalian species for the motifs containing the mutation site (dark arrow). The color spectrum represents the degree of amino acid conservation in these motifs.

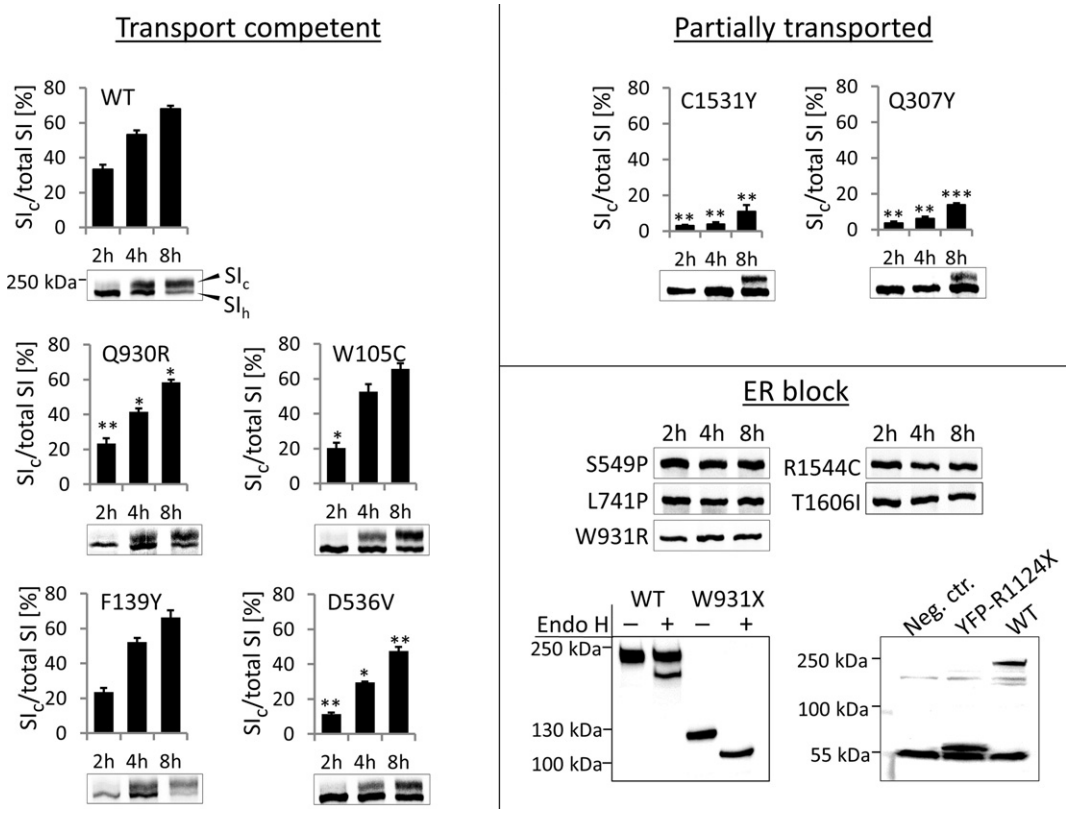

Fig. 2. Maturation rate of the SI mutants compared to the wild type SI. (A) Detection of SI from transiently transfected COS-1 cells after biosynthetic labeling. SI_h: immature mannose-rich form, SI_c: mature complex N- and O-glycosylated form, $n \geq 3$. The stop codon variants SI-W931X and SI-R1124X were transiently expressed in COS-1 cells and detected by immunoblotting. The SI-W931X mutant could be only detected in western blots as an ER-located endo H-sensitive protein and the SI-R1124X mutant was partially degraded in the cell and detectable only when tagged with YFP at its N-terminus.

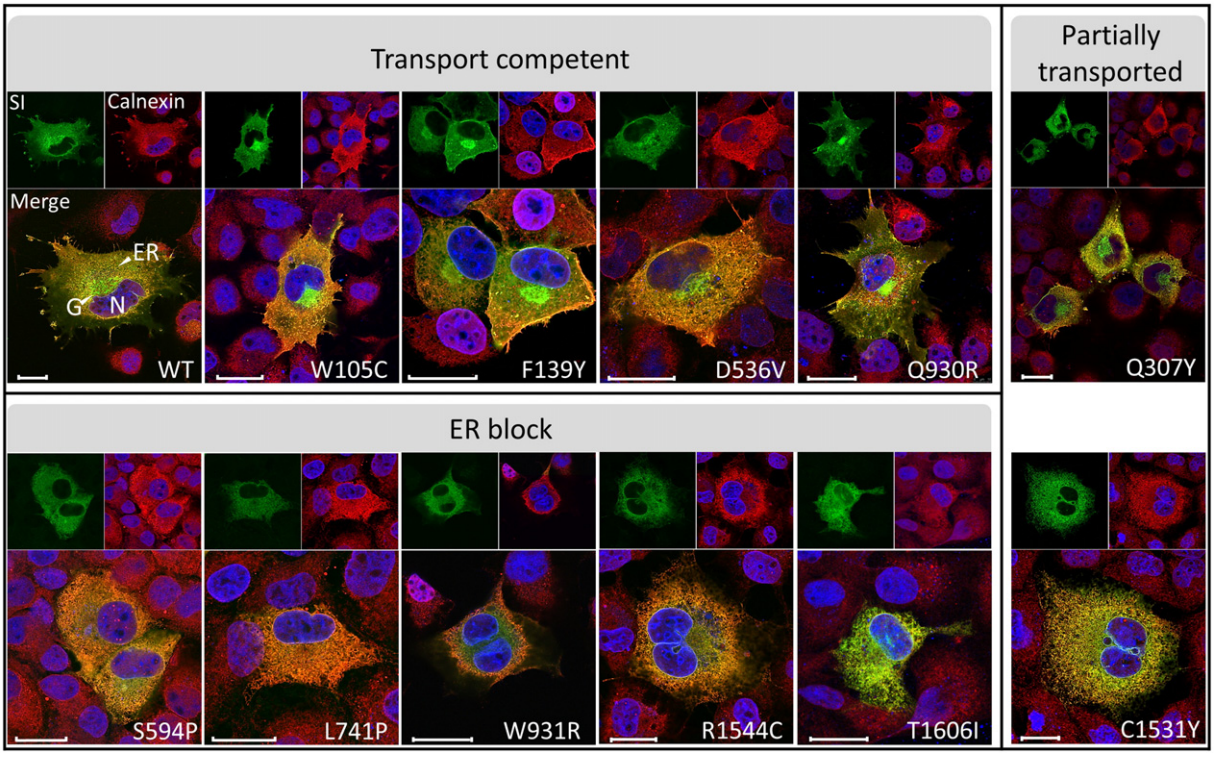

Fig. 3. Confocal microscope analysis of the SI wild type and mutants expressed in COS-1 cells. SI (green) was visualized in combination with the cell nucleus (blue) and endogenous calnexin (red) as an ER marker using indirect fluorescence. Scale bars: 25 μm, G: Golgi apparatus, N: nucleus.

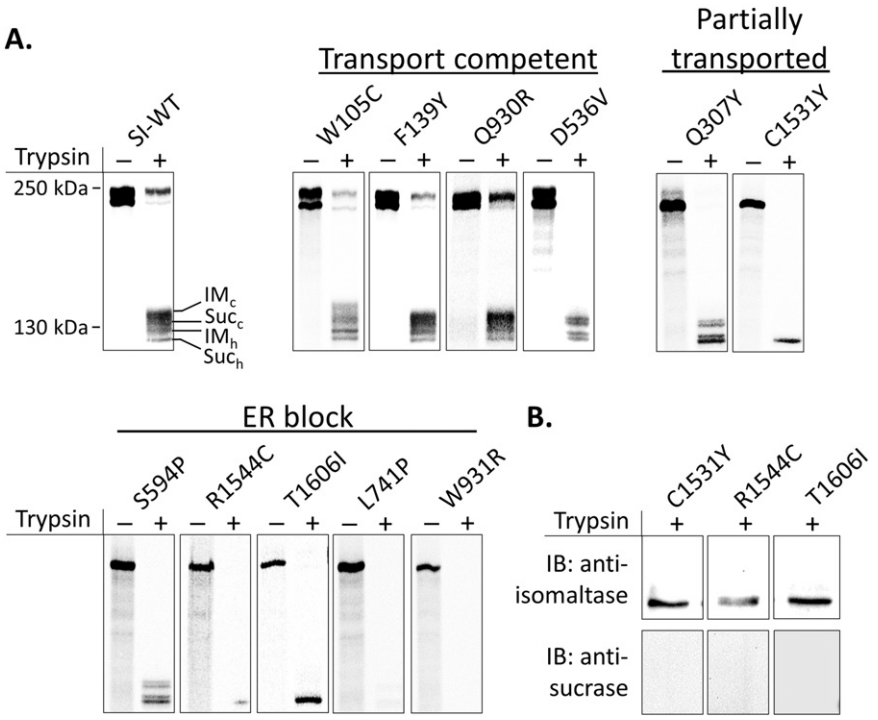

Fig. 4. Examination of the protein folding of the SI mutants by trypsin treatment. (A) After biosynthetic labeling and immunoprecipitation, the wild type and different mutants of SI were treated with 500 BAEE units trypsin for 1 h. IM_c/Suc_c: complex N- and O-glycosylated isomaltase and sucrase subunits, IM_h/Suc_h: mannose-rich forms of the isomaltase and sucrase subunits. (B) The single-band cleavage products of SI-C1531Y, SI-R1544C and SI-T1606I mutants were further characterized using differential immunoblotting of the trypsinized unlabeled material with anti-isomaltase (HBB3/705/60) or anti-sucrase (HBB2/614/88) monoclonal antibodies.

acquired complex glycosylation were associated to a large extent with the lipid rafts revealed in the floating fractions of the sucrose gradients. Other mutants displayed substantially lower levels or no incorporation into the lipid rafts (Fig. 5). Here, flotillin-2 in fractions 1–3 serves as a lipid raft marker [46] and Rho A in fractions 8–10 delineates the non-raft fractions. We conclude that the lipid raft association of SI variants correlate well with their maturation pattern and constitute another criterion that describes the impact of a particular mutation on the SI function.

In conclusion, the analyses of the SI variants at the biochemical and cell biological levels revealed three biosynthetic phenotypes (I–III). Phenotype I comprise SI mutants that showed comparable trafficking to wild type SI as well as virtually normal protein folding. The second phenotype, phenotype II, harbors two mutants with delayed trafficking and normal or partial folding. Phenotype III, the most severe one, includes mutants located in the ER that are either partially folded or completely misfolded.

3.3. Functional variations elicited by the mutations

The digestive capacities of the individual SI mutants were assessed *in vitro* and correlated with the sucrase (SUC) and isomaltase (IM) *ex vivo* activities measured in small bowel biopsies of CSID patients (Table 2). For this purpose, wild type SI or SI variants were purified by immunoprecipitation from the transiently transfected COS-1 cells and the SUC and IM specific activities were determined. Fig. 6 demonstrates that mutants from phenotype I and phenotype II showed reduced but varying enzymatic activities of SUC and IM. Only one of the mutants from phenotype I, Q930R, showed normal activities. Nearly all transport incompetent mutants

Table 3
Overview of the biochemical and functional features of the single SI variants compared to the wild type. A categorization of the SI mutants into 3 biosynthetic phenotypes was performed according to the influence of the respective mutation on the SI biochemical features and overall function.

	SI mutation	Domain of mutation	Maturation [%]	Isomaltase activity [%]	Sucrase activity [%]	Tryptic cleavage pattern	Lipid raft association [%]
WT	–	–	100	100	100	Normal	100
Biosynthetic phenotype I	W105C	Trefoil 1	96	61	30	Normal	92
	F139Y	Isomaltase	97	66	47	Normal	63
	Q930R	Isomaltase	87	98	102	Normal	107
	D536V	Isomaltase	70	1	58	Normal	77
Biosynthetic phenotype II	C1531Y	Sucrase	16	109	7	Part. degraded	35
	Q307Y	Isomaltase	20	2	22	Normal	42
Biosynthetic phenotype III	T1606I	Sucrase	0	76	19	Part. degraded	39
	R1544C	Sucrase	0	71	3	Part. degraded	30
	S594P	Isomaltase	0	4	4	Normal	20
	W931R	Isomaltase	0	11	11	Degraded	0.1
	L741P	Isomaltase	0	6	6	Degraded	0
	W931X	Isomaltase	0	0	0	Degraded	0
	R1124X	Sucrase	0	0	0	Degraded	0

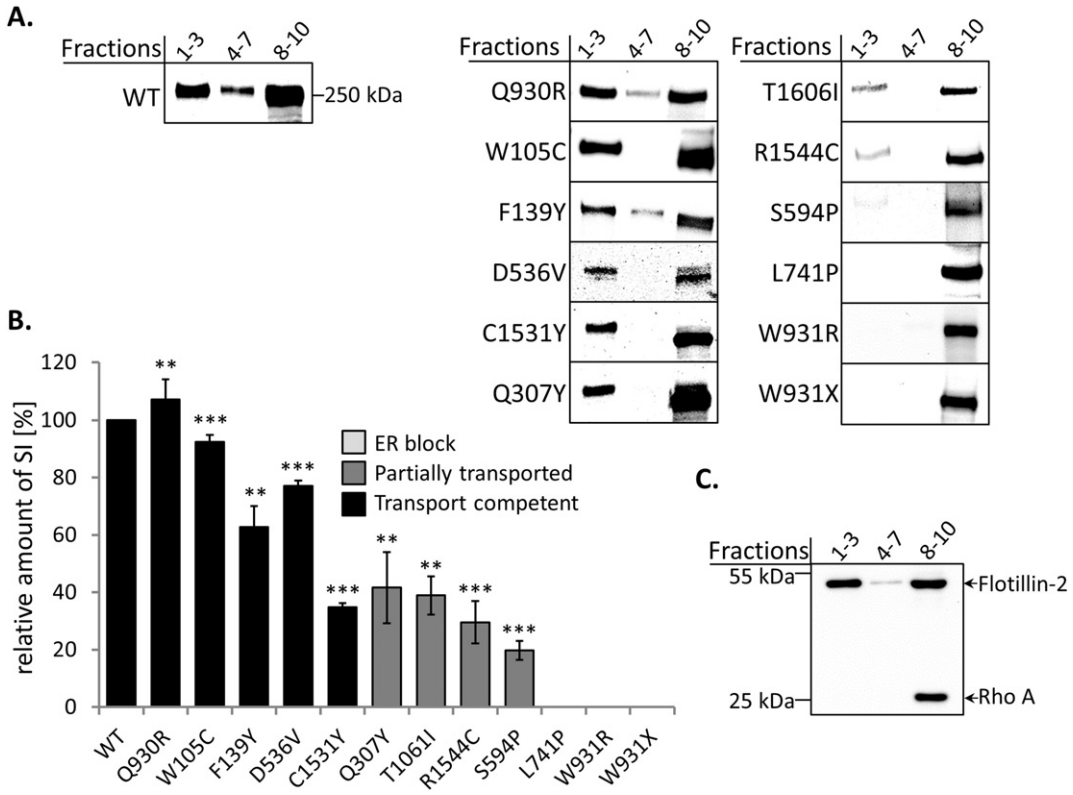

Fig. 5. Association of SI mutants with cholesterol-enriched membrane microdomains or lipid rafts. (A) Transiently transfected COS-1 cells were solubilized with 1% Lubrol WX and lipid raft and non-raft fractions were separated using sucrose density gradients. Lipid raft fractions (1–3) and non-raft fractions (4–7, 8–10) were pooled and analyzed by immunoblotting with anti-SI antibodies. (B) Graphical presentation of the lipid raft enrichment factor of SI mutants *versus* the wild type. The amount of wild type SI associated with lipid rafts was set to 100% and lipid raft association of the SI mutants was normalized to the wild type. (C) Representative control immunoblot for the lipid raft preparations illustrating the distribution of flotillin-2 which is mainly associated with lipid rafts and Rho A as a non-raft marker.

from phenotype III, S594P, L741P, W931R, W931X and R1124X, were also enzymatically inactive. The two remaining mutants from phenotype III, R1544C and T1606I, displayed isomaltase activity but cannot reach the cell surface due to their trafficking defect to fulfil their functions (Fig. 6). The loss of *in vitro* function of phenotype III mutants was reflected by the enzymatic activities measured in small bowel biopsies of the CSID patients (Table 2). Patients with inheritance of one mutation from phenotype III on each allele also showed a complete loss of intestinal SI activities *in vivo*. The combination of mutations from phenotype III with that of phenotype I or II in patients led to reduced but varying activities matching to a certain extent with our *in vitro* data (Table 2).

Notably, our *in vitro* modelling revealed that mutations in one subunit can also influence the activity of the other subunit most likely by

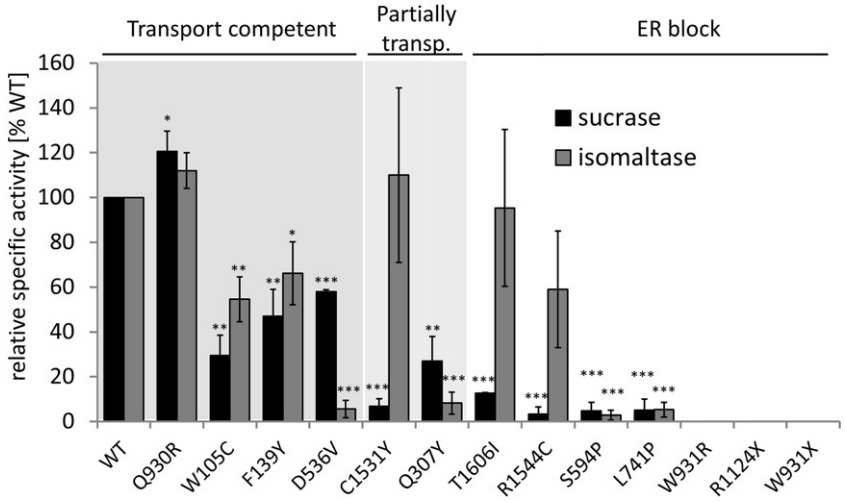

Fig. 6. Specific enzyme activities of the SI mutants *versus* wild type SI. Wild type or mutants of SI were immunoprecipitated from transfected COS-1 cells and assessed for sucrase and isomaltase activities. The relative SI content of each sample was determined by immunoblotting. Relative specific activities are recorded in comparison to wild type SI. SI mutants are grouped based on their similar trafficking characteristics.

imposing structural changes. Interestingly, mutations in the IM affected activities in both subunits and that in SUC mostly led to loss of the SUC activity, with preserved the IM activity.

The IM-located mutations, Q307Y and D536V, completely abolished the IM activity and substantially reduced the SUC activity. The SUC mutations on the other hand C1531Y, R1544C and T1606I were associated with complete reduction in SUC, while IM was either not affected or its activity was only slightly reduced (Fig. 6).

Moreover the detection of IM activity in some mannose-rich glycosylated transport incompetent mutants suggests that complex N- and O-glycosylation of IM is required for proper transport but not essentially for its enzyme activity. Nevertheless, the active enzyme will not be available at the cell surface, which is required for disaccharide digestion in the intestinal lumen.

4. Discussion

In the present study we have analyzed the pathobiochemistry of 13 naturally occurring missense mutations in SI, which have been identified in patients with CSID. This study has unraveled a remarkable heterogeneity in the molecular pathogenesis of CSID revealing the unique molecular etiologies of this multifaceted intestinal malabsorption disorder. CSID belongs to a group of protein folding diseases that can be triggered by improper folding like CFTR in cystic fibrosis and β-glucosidase in Gaucher disease [47–50], improper targeting and localization like AAT deficiency [51], dominant negative mutations like Keratin in epidermolysis bullosa simplex [52] or accumulation of aggregated proteins like amyloid accumulation [53]. Unlike many of the aforementioned diseases, however, multiple mechanisms can elicit CSID rendering this intestinal disorder unique among other protein folding diseases. In fact, mutations identified in patients of CSID are associated with severe biosynthetic phenotypes of altered folding, aberrant trafficking, missorting and even functional deficits in a correctly folded protein [26,31–33,54].

The molecular and cellular analyses of these 13 novel mutants have led to the categorization of CSID into three major biosynthetic phenotypes based on criteria that comprised protein trafficking, enzyme function and lipid raft association of SI mutants (Fig. 8).

The first group of mutants includes W105C, F139Y, D536V and Q930R with comparable maturation rates to wild type SI. These mutants do not reveal gross structural alterations and are properly trafficked along the secretory pathway, but not necessarily to the cell surface. The normal maturation is not always associated with normal activity levels. In fact, while the Q930R mutant is almost as active as wild type SI, the remaining mutants of this category reveal reduced activities of down to 30% *versus* the wild type SI (Table 3).

The second group includes Q307Y and C1531Y and is characterized by delayed maturation and reduced digestive capacities. The third group consists of L741P, S594P, R1544C, T1606I, W931R, W931X, and R1124X and constitutes the most severe effect on the SI function *in vitro*. The major characteristics of the mutants in this group are their intracellular block in the ER as immature mannose-rich glycosylated forms as well as the functional deficits with complete loss of sucrase and isomaltase activities. The residual enzymatic activities of a few mutants cannot be made accessible to the substrate *in vivo* due to the failure of these mutants to reach the cell surface. In particular the complete loss of function of mutations grouped into the phenotype III indicates a high molecular pathogenicity of these mutants.

The classification of the mutants into three groups may provide an explanation for the variations in the enzymatic activities and subsequently the underlying pathomechanisms that elicit severe, intermediate or mild symptoms in several cases of CSID. While the level of severity in CSID cases elicited by compound heterozygous mutations belonging to phenotype III would be expected to be the highest, a combination of a mutation of phenotype III, for example R1544C with a mutation from phenotype I Q930R may generate a milder form of CSID. In fact, measurements of the enzyme activity levels support this view.

The current data propose that the pathogenesis of CSID is a multifactorial network of events that altogether elicit the wide heterogeneity in the overall pattern of CSID. The biosynthetic, trafficking, functional features as well as the lipid raft association of the individual mutants comprise most essential elements in the regulation of the carbohydrate digestive capacity of the SI isoforms. Nevertheless, the degree of a putative regulatory influence of these mutants on each other in compound heterozygosity should be addressed. Particularly in cases when mutants with wild type-like trafficking behaviour are co-expressed with highly pathogenic ER-located mutants a potential interaction of the mutants with ultimate influence on their subsequent targeting along the secretory pathway and functional characteristics can be anticipated. In fact, SI is a type II membrane glycoprotein and an SI monomer may interact with another SI monomer in an oligomer-like fashion similar to that described for type II membrane proteins of the *medial*-Golgi and referred to as kin recognition [55]. This mode of interaction is supported by the fact that SI acquires dimeric topology along the secretory pathway [56] and retains this topology at the brush border membrane [57] (Fig. 7).

Another factor that offers an explanation for the wide variations in the SI activities in compound heterozygote subjects is the mosaic expression pattern of the disaccharidases including SI. Regardless of any abnormalities in the structure or function of SI, the gene expression of this enzyme can be downregulated in different regions of the intestinal epithelium that is ultimately associated with reduced carbohydrate digestion capacity of the intestine [58,59]. Hitherto individuals with an *a priori* reduced expression of wild type SI will be more susceptible to develop gastrointestinal symptoms in a heterozygote background. This possibility is similar to a haploinsufficiency model, in which one gene allele produces low levels of a functionally active protein, while the other allele is pathogenic. The difference, however, to the mosaic expression pattern of SI is the heterogeneous expression levels of wild type SI in the enterocytes that vary from low to normal [58].

Current concepts have established CSID to be inherited as homozygous or compound heterozygous traits [22]. Interestingly, a study with a cohort of Hungarian patients suffering from symptoms similar to those in CSID patients revealed that 5 out of 11 subjects are heterozygotes for the severe mutations G1073D, F1745C, C1229Y and T694P [9]. The high frequency of heterozygotes in the Hungarian patients suggests that heterozygous insufficiency is a potentially novel phenotype of CSID. The fact that the mutants with this pattern of inheritance are highly pathogenic suggests that an interaction between a wild type SI and one of these mutants may downregulate the activity of the wild type

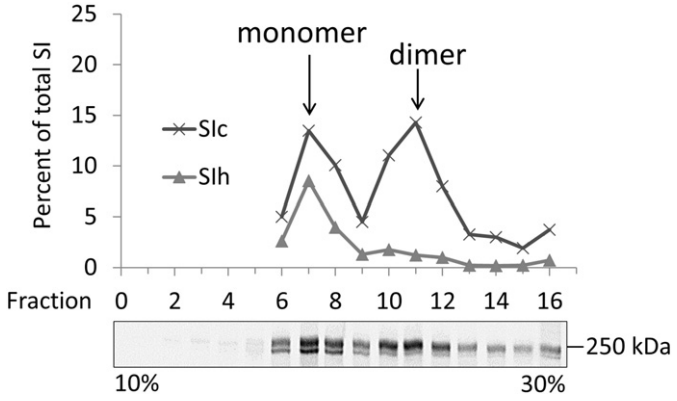

Fig. 7. Quaternary structure of sucrase-isomaltase. The complex glycosylated biosynthetic form of SI is revealed in two peaks of the gradient compatible with two different quaternary structures. SI_h: immature mannose-rich form, SI_c: mature complex N- and O-glycosylated form.

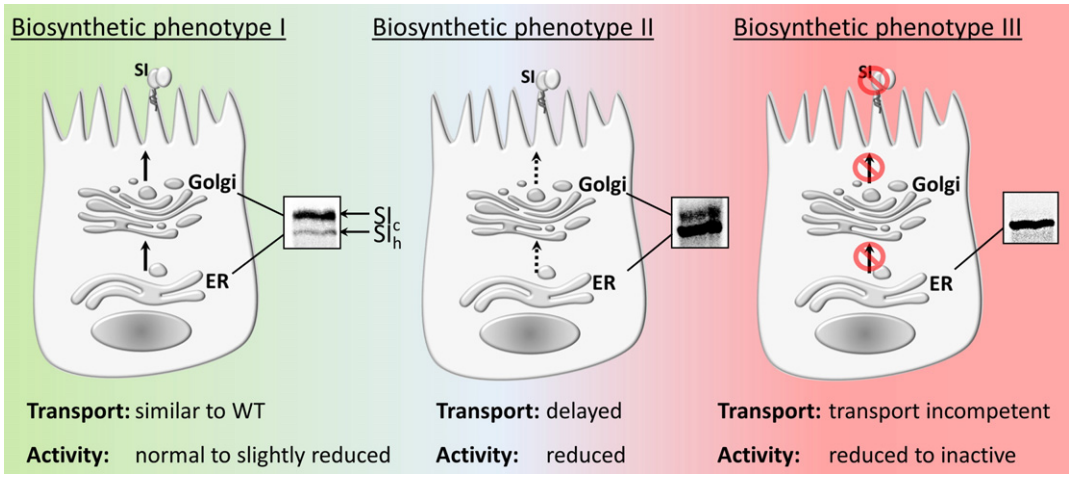

Fig. 8. Classification of SI variants into three major biosynthetic phenotypes. In this model SI mutants are classified based on their molecular and functional characteristics *in vitro*. For expression of functional SI at the brush border membrane of the intestinal epithelium, the polypeptide should be properly folded, complex N- and O-glycosylated along the secretory pathway and sorted to the apical cell surface *via* association with cholesterol- and sphingolipid-enriched membrane microdomains. The intracellular trafficking behaviour of the mutants within the enterocyte is depicted. Representative radioactive micrographs show the maturation of SI. SI_c: complex N- and O-glycosylated SI; SI_h: mannose-rich immature form of SI.

substantially in the formed oligomer. As a consequence, SI-related malabsorption could be considered to be a more common disorder than initially thought. Nevertheless, this pattern of inheritance requires more detailed analyses at the molecular and cellular levels to establish itself as an independent novel class of CSID.

In conclusion, the current study supports the existence of heterogeneous forms of CSID that vary in their degree of enzymatic activity and probably clinical severity in light of a homozygous and compound heterozygote inheritance pattern. The mild to severe gradient in the SI function due to the mutants supports the view that a proper diagnosis of CSID could presumably be missed in several cases and introduces a new paradigm into CSID, which seems to occur in more individuals than initially thought.

Grant support

This work was partially supported by QOL Medical LLC, Vero Beach, Florida, USA and intramural funds from the University of Veterinary Medicine Hannover, Germany (both to HYN).

Financial disclosure, writing assistance and transcript profiling

Hassan Y. Naim has received an unrestricted research support from QOL Medical, Vero Beach, Florida and consultancy fee for reviewing research projects supported by the same company.

No conflicts of interest exist.

Author contributions

BG and MA performed the experiments, interpreted results and drafted the manuscript. CRS provided patients' data and revised the manuscript. HYN designed the study, interpreted results and drafted the manuscript.

Transparency document

The Transparency document associated with this article can be found, in the online version.

References

[1] M.B. Heyman, N. Comm, Lactose intolerance in infants, children, and adolescents, Pediatrics 118 (2006) 1279–1286.
[2] H.Y. Naim, E.E. Sterchi, M.J. Lentze, Biosynthesis of the human sucrase-isomaltase complex. Differential O-glycosylation of the sucrase subunit correlates with its position within the enzyme complex, J. Biol. Chem. 263 (1988) 7242–7253.
[3] H.Y. Naim, E.E. Sterchi, M.J. Lentze, Structure, biosynthesis, and glycosylation of human small intestinal maltase-glucoamylase, J. Biol. Chem. 263 (1988) 19709–19717.
[4] H.Y. Naim, E.E. Sterchi, M.J. Lentze, Biosynthesis and maturation of lactase-phlorizin hydrolase in the human small intestinal epithelial cells, Biochem. J. 241 (1987) 427–443.
[5] A.H. Lin, B.R. Hamaker, B.L. Nichols Jr., Direct starch digestion by sucrase-isomaltase and maltase-glucoamylase, J. Pediatr. Gastroenterol. Nutr. 55 (Suppl. 2) (2012) S43–S45.
[6] L. Sim, C. Willemsma, S. Mohan, et al., Structural basis for substrate selectivity in human maltase-glucoamylase and sucrase-isomaltase N-terminal domains, J. Biol. Chem. 285 (2010) 17763–17770.
[7] B.L. Nichols, S.E. Avery, W. Karnsakul, et al., Congenital maltase-glucoamylase deficiency associated with lactase and sucrase deficiencies, J. Pediatr. Gastroenterol. Nutr. 35 (2002) 573–579.
[8] M. Alfalah, R. Jacob, U. Preuss, et al., O-linked glycans mediate apical sorting of human intestinal sucrase-isomaltase through association with lipid rafts, Curr. Biol. 9 (1999) 593–596.
[9] P. Sander, M. Alfalah, M. Keiser, et al., Novel mutations in the human sucrase-isomaltase gene (SI) that cause congenital carbohydrate malabsorption, Hum. Mutat. 27 (2006) 119.
[10] M. Alfalah, M. Keiser, T. Leeb, et al., Compound heterozygous mutations affect protein folding and function in patients with congenital sucrase-isomaltase deficiency, Gastroenterology 136 (2009) 883–892.
[11] W.R. Treem, Clinical aspects and treatment of congenital sucrase-isomaltase deficiency, J. Pediatr. Gastroenterol. Nutr. 55 (Suppl. 2) (2012) S7–13.
[12] W.R. Treem, Congenital sucrase-isomaltase deficiency, J. Pediatr. Gastroenterol. Nutr. 21 (1995) 1–14.
[13] I. Antonowicz, J.D. Lloyd-Still, K.T. Khaw, et al., Congenital sucrase-isomaltase deficiency. Observations over a period of 6 years, Pediatrics 49 (1972) 847–853.
[14] P. Layer, A.R. Zinsmeister, E.P. Dimagno, Effects of decreasing intraluminal amylase activity on starch digestion and postprandial gastrointestinal function in humans, Gastroenterology 91 (1986) 41–48.
[15] T. Newton, M.S. Murphy, I.W. Booth, Glucose polymer as a cause of protracted diarrhea in infants with unsuspected congenital sucrase-isomaltase deficiency, J. Pediatr. 128 (1996) 753–756.
[16] K. Mikko, B. Ralf, R. Heli, et al., Lactase persistence and ovarian carcinoma risk in Finland, Poland and Sweden, Int. J. Cancer 117 (2005) 90–94.
[17] L. Vallaeys, S. Van Biervliet, G. De Bruyn, et al., Congenital glucose-galactose malabsorption: a novel deletion within the SLC5A1 gene, Eur. J. Pediatr. 172 (2013) 409–411.
[18] G. Samasca, M. Bruchental, A. Butnariu, et al., Difficulties in celiac disease diagnosis in children — a case report, Maedica (Buchar) 6 (2011) 32–35.
[19] N.A. Hering, A. Fromm, J. Kikhney, et al., *Yersinia enterocolitica* affects intestinal barrier function in the colon, J. Infect. Dis. 213 (2016) 1157–1162.

[20] G. Terrin, R. Tomaiuolo, A. Passariello, et al., Congenital diarrheal disorders: an updated diagnostic approach, Int. J. Mol. Sci. 13 (2012) 4168–4185.
[21] W.R. Treem, Clinical heterogeneity in congenital sucrase-isomaltase deficiency, J. Pediatr. 128 (1996) 727–729.
[22] H.Y. Naim, M. Heine, K.P. Zimmer, Congenital sucrase-isomaltase deficiency: heterogeneity of inheritance, trafficking, and function of an intestinal enzyme complex, J. Pediatr. Gastroenterol. Nutr. 55 (Suppl. 2) (2012) S13–S20.
[23] B.R. Hamaker, B.H. Lee, R. Quezada-Calvillo, Starch digestion and patients with congenital sucrase-isomaltase deficiency, J. Pediatr. Gastroenterol. Nutr. 55 (Suppl. 2) (2012) S24–S28.
[24] H.Y. Naim, J. Roth, E.E. Sterchi, et al., Sucrase-isomaltase deficiency in humans. Different mutations disrupt intracellular transport, processing, and function of an intestinal brush border enzyme, J. Clin. Invest. 82 (1988) 667–679.
[25] J.A. Fransen, H.P. Hauri, L.A. Ginsel, et al., Naturally occurring mutations in intestinal sucrase-isomaltase provide evidence for the existence of an intracellular sorting signal in the isomaltase subunit, J. Cell Biol. 115 (1991) 45–57.
[26] R. Jacob, K.P. Zimmer, J. Schmitz, et al., Congenital sucrase-isomaltase deficiency arising from cleavage and secretion of a mutant form of the enzyme, J. Clin. Invest. 106 (2000) 281–287.
[27] E. Gudmand-Hoyer, H.J. Fenger, P. Kern-Hansen, et al., Sucrase deficiency in Greenland. Incidence and genetic aspects, Scand. J. Gastroenterol. 22 (1987) 24–28.
[28] M.L. Peterson, R. Herber, Intestinal sucrase deficiency, Trans. Assoc. Am. Phys. 80 (1967) 275–283.
[29] J.D. Welsh, J.R. Poley, M. Bhatia, et al., Intestinal disaccharidase activities in relation to age, race, and mucosal damage, Gastroenterology 75 (1978) 847–855.
[30] S. Uhrich, Z. Wu, J.Y. Huang, et al., Four mutations in the SI gene are responsible for the majority of clinical symptoms of CSID, J. Pediatr. Gastroenterol. Nutr. 55 (Suppl. 2) (2012) S34–S35.
[31] V. Ritz, M. Alfalah, K.P. Zimmer, et al., Congenital sucrase-isomaltase deficiency because of an accumulation of the mutant enzyme in the endoplasmic reticulum, Gastroenterology 125 (2003) 1678–1685.
[32] M. Keiser, M. Alfalah, M.J. Propsting, et al., Altered folding, turnover, and polarized sorting act in concert to define a novel pathomechanism of congenital sucrase-isomaltase deficiency, J. Biol. Chem. 281 (2006) 14393–14399.
[33] M.J. Propsting, R. Jacob, H.Y. Naim, A glutamine to proline exchange at amino acid residue 1098 in sucrase causes a temperature-sensitive arrest of sucrase-isomaltase in the endoplasmic reticulum and *cis*-Golgi, J. Biol. Chem. 278 (2003) 16310–16314.
[34] H.P. Hauri, E.E. Sterchi, D. Bienz, et al., Expression and intracellular transport of microvillus membrane hydrolases in human intestinal epithelial cells, J. Cell Biol. 101 (1985) 838–851.
[35] J.F. Beaulieu, B. Nichols, A. Quaroni, Posttranslational regulation of sucrase-isomaltase expression in intestinal crypt and villus cells, J. Biol. Chem. 264 (1989) 20000–20011.
[36] B.E. Slatko, J. Kieleczawa, J. Ju, et al., "First generation" automated DNA sequencing technology, Curr. Protoc. Mol. Biol. (2011) (Chapter 7:Unit7.2).
[37] J. Ouwendijk, C.E. Moolenaar, W.J. Peters, et al., Congenital sucrase-isomaltase deficiency. Identification of a glutamine to proline substitution that leads to a transport block of sucrase-isomaltase in a pre-Golgi compartment, J. Clin. Investig. 97 (1996) 633641.
[38] H.Y. Naim, S.W. Lacey, J.F. Sambrook, et al., Expression of a full-length cDNA coding for human intestinal lactase-phlorizin hydrolase reveals an uncleaved, enzymatically active, and transport-competent protein, J. Biol. Chem. 266 (1991) 12313–12320.
[39] R. Jacob, K. Peters, H.Y. Naim, The prosequence of human lactase-phlorizin hydrolase modulates the folding of the mature enzyme, J. Biol. Chem. 277 (2002) 8217–8225.
[40] R. Jacob, J.R. Weiner, S. Stadge, et al., Additional N-glycosylation and its impact on the folding of intestinal lactase-phlorizin hydrolase, J. Biol. Chem. 275 (2000) 10630–10637.
[41] N. Spodsberg, R. Jacob, M. Alfalah, et al., Molecular basis of aberrant apical protein transport in an intestinal enzyme disorder, J. Biol. Chem. 276 (2001) 23506–23510.
[42] M. Amiri, H.Y. Naim, Long term differential consequences of miglustat therapy on intestinal disaccharidases, J. Inherit. Metab. Dis. 37 (2014) 929–937.
[43] E. Fic, S. Kedracka-Krok, U. Jankowska, et al., Comparison of protein precipitation methods for various rat brain structures prior to proteomic analysis, Electrophoresis 31 (2010) 3573–3579.
[44] S. Schmidt, G. Fracasso, M. Colombatti, et al., Cloning and characterization of canine prostate-specific membrane antigen, Prostate 73 (2013) 642–650.
[45] V.A. Simossis, J. Heringa, PRALINE: a multiple sequence alignment toolbox that integrates homology-extended and secondary structure information, Nucleic Acids Res. 33 (2005) W289–W294.
[46] Y. Sasaki, Y. Oshima, R. Koyama, et al., Identification of flotillin-2, a major protein on lipid rafts, as a novel target of p53 family members, Mol. Cancer Res. 6 (2008) 395–406.
[47] A. Piepoli, E. Schirru, A. Mastrorilli, et al., Genotyping of the lactase-phlorizin hydrolase c/t-13910 polymorphism by means of a new rapid denaturing high-performance liquid chromatography-based assay in healthy subjects and colorectal cancer patients, J. Biomol. Screen. 12 (2007) 733–739.
[48] K. Du, M. Sharma, G.L. Lukacs, The DeltaF508 cystic fibrosis mutation impairs domain-domain interactions and arrests post-translational folding of CFTR, Nat. Struct. Mol. Biol. 12 (2005) 17–25.
[49] B.H. Qu, E.H. Strickland, P.J. Thomas, Localization and suppression of a kinetic defect in cystic fibrosis transmembrane conductance regulator folding, J. Biol. Chem. 272 (1997) 15739–15744.
[50] I. Ron, M. Horowitz, ER retention and degradation as the molecular basis underlying Gaucher disease heterogeneity, Hum. Mol. Genet. 14 (2005) 2387–2398.
[51] D.A. Lomas, D.L. Evans, J.T. Finch, et al., The mechanism of Z alpha 1-antitrypsin accumulation in the liver, Nature 357 (1992) 605–607.
[52] N.S. Werner, R. Windoffer, P. Strnad, et al., Epidermolysis bullosa simplex-type mutations alter the dynamics of the keratin cytoskeleton and reveal a contribution of actin to the transport of keratin subunits, Mol. Biol. Cell 15 (2004) 990–1002.
[53] C. Glabe, Intracellular mechanisms of amyloid accumulation and pathogenesis in Alzheimer's disease, J. Mol. Neurosci. 17 (2001) 137–145.
[54] H.P. Hauri, J. Roth, E.E. Sterchi, et al., Transport to cell surface of intestinal sucrase-isomaltase is blocked in the Golgi apparatus in a patient with congenital sucrase-isomaltase deficiency, Proc. Natl. Acad. Sci. 82 (1985) 4423–4427.
[55] T. Nilsson, P. Slusarewicz, M.H. Hoe, et al., Kin recognition. A model for the retention of Golgi enzymes, FEBS Lett. 330 (1993) 1–4.
[56] E.M. Danielsen, Dimeric assembly of enterocyte brush border enzymes, Biochemistry 33 (1994) 1599–1605.
[57] G.M. Cowell, J. Tranum-Jensen, H. Sjostrom, et al., Topology and quaternary structure of pro-sucrase/isomaltase and final-form sucrase/isomaltase, Biochem. J. 237 (1986) 455–461.
[58] K. Reinshagen, K.M. Keller, B. Haase, et al., Mosaic pattern of sucrase isomaltase deficiency in two brothers, Pediatr. Res. 63 (2008) 79–83.
[59] B.L. Nichols, F. Carrazza, V.N. Nichols, et al., Mosaic expression of brush-border enzymes in infants with chronic diarrhea and malnutrition, J. Pediatr. Gastroenterol. Nutr. 14 (1992) 371–379.
[60] A. Dahlqvist, Assay of intestinal disaccharidases, Scand. J. Clin. Lab. Invest. 44 (1984) 169–172.
[61] S.K. Gupta, S.K. Chong, J.F. Fitzgerald, Disaccharidase activities in children: normal values and comparison based on symptoms and histologic changes, J. Pediatr. Gastroenterol. Nutr. 28 (1999) 246–251.